Check for updates

Received: 9 January 2022 | Revised: 26 August 2022 | Accepted: 30 August 2022

DOI: 10.1111/ejn.15824

RESEARCH REPORT

EJN European Journal of Neuroscience FENS WILEY

WildLab: A naturalistic free viewing experiment reveals previously unknown electroencephalography signatures of face processing

Anna L. Gert[1] | Benedikt V. Ehinger[2,3] | Silja Timm[1] | Tim C. Kietzmann[2,4] | Peter König[1,5]

[1]Institute of Cognitive Science, Osnabrück University, Osnabrück, Germany

[2]Donders Institute for Brain, Cognition and Behaviour, Radboud University, Nijmegen, The Netherlands

[3]Stuttgart Center for Simulation Science, University of Stuttgart, Stuttgart, Germany

[4]MRC Cognition and Brain Sciences Unit, Cambridge University, Cambridge, UK

[5]Department of Neurophysiology and Pathophysiology, University Medical Center Hamburg-Eppendorf, Hamburg, Germany

Correspondence
Anna L. Gert, Institute of Cognitive Science, Osnabrück University, Osnabrück, Germany.
Email: agert@uos.de

Funding information
Deutsche Forschungsgemeinschaft, Grant/Award Number: EXC2075 - 390740016; H2020 Future and Emerging Technologies, Grant/Award Number: SEP-210141273

Edited by: Guillaume Rousselet

Abstract

Neural mechanisms of face perception are predominantly studied in well-controlled experimental settings that involve random stimulus sequences and fixed eye positions. Although powerful, the employed paradigms are far from what constitutes natural vision. Here, we demonstrate the feasibility of ecologically more valid experimental paradigms using natural viewing behaviour, by combining a free viewing paradigm on natural scenes, free of photographer bias, with advanced data processing techniques that correct for overlap effects and co-varying non-linear dependencies of multiple eye movement parameters. We validate this approach by replicating classic N170 effects in neural responses, triggered by fixation onsets (fixation event-related potentials [fERPs]). Importantly, besides finding a strong correlation between both experiments, our more natural stimulus paradigm yielded smaller variability between subjects than the classic setup. Moving beyond classic temporal and spatial effect locations, our experiment furthermore revealed previously unknown signatures of face processing: This includes category-specific modulation of the event-related potential (ERP)'s amplitude even before fixation onset, as well as adaptation effects across subsequent fixations depending on their history.

KEYWORDS
event-related potentials (ERPs), eye movements, face processing, fixation-related potentials, natural images

1 | INTRODUCTION

The electroencephalography (EEG) correlates of face processing have been studied widely over the last decades, as faces represent an important stimulus category in our everyday life. Using well-controlled

Abbreviations: EEG, electroencephalography; ERP, event-related potential; ET, eye-eyetracking; fERP, fixation event-related potential; TFCE, threshold-free cluster enhancement.

Tim C. Kietzmann and Peter König shared senior authorship.

This is an open access article under the terms of the Creative Commons Attribution License, which permits use, distribution and reproduction in any medium, provided the original work is properly cited.
© 2022 The Authors. *European Journal of Neuroscience* published by Federation of European Neuroscience Societies and John Wiley & Sons Ltd.

experimental paradigms, numerous studies have revealed a face-specific modulation of event-related potentials (ERPs) that occur in occipito-temporal electrodes around 170 ms after stimulus onset (N170) (Bentin et al., 1996). Most studies (Eimer, 2011; Itier & Taylor, 2004; Rossion & Jacques, 2008; but also see Thierry et al., 2007) report this component to be more negative for trials that presented a face, in comparison with other categories like cars, butterflies or clocks (Rossion & Jacques, 2008).

Although the N170 is a highly robust experimental finding, most of what we know about the neural correlates of face processing is derived from 'classic' experimental paradigms derived to enable maximal control over stimulus parameters. These include stimulus' contrast (Itier & Taylor, 2004), spatial frequency (Goffaux et al., 2003), inversion (Rossion et al., 2000), shape (Dering et al., 2011), integrity (George et al., 1996) or orientation (Kietzmann et al., 2016). Although more natural stimulus material with varying perspectives and backgrounds (Cauchoix et al., 2014; Rousselet et al., 2004) or movement (Johnston et al., 2015) have successfully been used to produce face-related EEG responses, most experimental setups remain highly artificial. For example, they rely on randomized sequences of stimulus presentations and do not allow for eye movements, although the latter play a central role in natural vision.

Fixation-related potentials have been used previously to investigate face processing in an unrestricted viewing paradigm (Auerbach-Asch et al., 2020). To study the relationship between passive and active vision, the authors presented cutouts of faces in front of a noisy background. The faces were presented in small panels at the screen's corners and responses were compared with similar-shaped painted eggs in a passive condition, a cued condition and an eye movement condition in which participants had to count the number of faces present. Although this gives us a first controlled insight into face processing under more natural conditions, it remains unknown how the view of full faces is processed in a natural context and under unconstrained free viewing conditions.

A potential consequence that comes into play in free viewing studies is sequential effects. Previously, these effects have been well described, for instance, in choice biases in behaviour (Akaishi et al., 2014; Bosch et al., 2020; Fischer & Whitney, 2014), pupil dilation (Urai et al., 2017) or face identity perception (Liberman et al., 2014). However, there are also direct effects, that is, autocorrelations, within sequences of eye movements. One prominent example is the overabundance of forward saccades (Wilming et al., 2013). Effects of such serial dependencies on neuronal activity have been found to occur in early visual areas (John-Saaltink et al., 2016) and higher cortical areas. In an EEG study, Körner et al. (2014) even showed sequential effects for fixation locked ERPs in a visual search task. We will analyse the sequential effect of fixation history on face processing by explicitly modelling the fixation history at the previous fixation locations.

Here, we advance the study of face perception by introducing an experimental and analysis paradigm that allows for active vision on natural scenes. This is accomplished by a combination of three elements. First, we perform simultaneous recordings of eye movements and electrophysiological data. Second, we use an unrestricted free viewing paradigm on natural stimuli (WildLab), sampled without photographer bias from an HD head-cam that volunteers wore while moving in the real world. Third, we employ a novel analysis pipeline of fixation ERPs (fERPs) that is capable of controlling for temporal overlap in neural processes elicited by rapidly occurring eye movements as well as disentangling and adjusting for the effects of varying eye movement parameters.

Previewing our results, we demonstrate a high within-subject correlation of N170 effect sizes across free viewing and a classic experimental paradigm, validating our approach. Importantly, we observe a reduction in the effect size and its variance across subjects for free viewing, indicating that the more natural setup led to more consistent brain activity. Furthermore, in comparison with fixations on the background, the WildLab condition shows a modulation already at the P100. Moreover, we also find evidence for sequential effects in subsequent fERPs, emerging even before fixation onset. These findings highlight the importance of understanding eye movements as a sequence of peripheral preview and foveated analysis and not as a series of independent, rapid stimulus onsets and add further support for utilizing more natural stimulus paradigms.

2 | METHODS

2.1 | Participants

Twenty-three participants took part in our experiment. We excluded three subjects from further analyses. For one, we could not synchronize the ET and EEG data. For the other two, the eye-tracking (ET) data were not usable due to technical problems.

All 20 participants (15 females and 5 males; age: 19 to 31) reported normal or corrected to normal visual acuity. Participants gave written consent and were unaware of the purpose of the study. They received an hourly reward of either €8.84 or course credits. The study was approved

14609568, 2022, 11, Downloaded from https://onlinelibrary.wiley.com/doi/10.1111/ejn.15824 by Universitatsbibliothek Stuttgart, Wiley Online Library on [27/05/2024]. See the Terms and Conditions (https://onlinelibrary.wiley.com/terms-and-conditions) on Wiley Online Library for rules of use; OA articles are governed by the applicable Creative Commons License

by the local ethics committee (Osnabrück University, 55/10).

2.2 | Technical setup

EEG data were recorded using a 128 Ag/AgCl-electrode system placed according to the 5% international system using a WaveGuard cap (ANT, Netherlands) and two Refa8 (TMSi, Netherlands) amplifiers. We recorded with a sampling rate of 1024 Hz and used electrode Cz as the reference. The ground electrode was placed under the left collarbone. Eye movements were recorded via electrooculogram (EOG) with a bipolar electrode being placed above and below the left eye. Impedances were kept below 10 kΩ.

Eye movements were recorded using an EyeLink 1000 remote eye tracker (EyeLink, SR Research, Canada) with a sampling frequency of 500 Hz in remote mode. For the ClassicLab condition, we used a nine-point calibration before the first and fifth block. For the WildLab condition, we calibrated before the first, fourth and seventh experimental block. The average calibration error was kept below .5° visual angle with a maximum error of 1.0°.

We used a large presentation screen with a width of 64″ and a height of 36″ (PA328Q, Asus, Taipei, Taiwan), a resolution of 3840 × 2160 pixels and a refresh rate of 60 Hz. A luminance sensor was attached to the bottom left corner of the screen to detect changes in the monitor (i.e., stimulus onset and offset). This was done to compensate for time delays between the trigger and the actual stimulus onsets. All data were corrected for this time delay. A jitter in this temporal delay was not found.

2.3 | Procedure

Participants were seated in a dimly lit room with their heads centred to the presentation screen at a distance of approximately 80 cm, without a chinrest.

The order of experiments was balanced between participants to avoid sequential task biases. Each experiment took about 40 to 60 min, including self-paced breaks after each block. The whole session including the EEG setup took about 3 to 4 h.

2.4 | ClassicLab passive viewing

2.4.1 | Stimuli

During the ClassicLab condition, faces (front on, or 40° rotation to the left or right), objects and cars were shown. For each stimulus category, we used 20 different identities. The face pictures were taken from a database of coworkers working at the NeuroBioPsychology Group of Osnabrück University. This database consists of photographs of 10 males and 10 females with neutral facial expressions, wearing black T-shirts with varying hair colours and styles from several different angles. Object photographs were taken from the Konkle's Big and Small Objects database (Konkle & Caramazza, 2013) with 10 small and 10 large objects. Twenty car photographs were taken from Krause et al. (2013). These photographs depicted a range of different car types of various colours and shapes.

We matched the number of white pixels of each stimulus, but no other low-level features. Pictures could, therefore, vary in size. All stimuli were presented centrally on a bright white background. Car trials were part of a different research question and are not analysed here.

2.4.2 | Experimental design

Each passive viewing trial consisted of a fixation dot presented for 300 ms followed by a stimulus presented for 300 ms (Figure 1), followed by a white blank screen with an inter-trial interval of 1300 ms (uniform jitter of 1200–1400 ms).

We presented 1280 trials, where each of the 80 stimuli was presented 16 times randomly across eight blocks, except the left and right half-profile stimuli, which were each repeated only 8 times per block. In total, there are 320 trials for each condition. The order of stimulus presentation within each block was pseudo-randomized, with no direct repetition of the same picture to avoid repetition effects. After every block, subjects were allowed to take a break.

2.5 | WildLab free viewing

2.5.1 | Natural stimuli

The stimulus set comprises scenes taken inside a local shopping centre (Lengermann + Trieschmann, Osnabrück, Germany). To avoid the photographer's bias, we recorded video streams with a GoPro camera (ASST1, Hero 5, GoPro, Inc., CA, USA) mounted on the head of a participant piloting a mobile version of this experiment. The subject was freely moving inside the mall wearing a mobile EEG and ET setup and was given the task to explore.

We extracted single frames from the recorded video streams. In a first step, these frames were then manually

14609568, 2022, 11, Downloaded from https://onlinelibrary.wiley.com/doi/10.1111/ejn.15824 by Universitatsbibliothek Stuttgart, Wiley Online Library on [27/05/2024]. See the Terms and Conditions (https://onlinelibrary.wiley.com/terms-and-conditions) on Wiley Online Library for rules of use; OA articles are governed by the applicable Creative Commons License

FIGURE 1 Exemplary trial and stimuli. (a) Trial structure of the classic, passive condition (ClassicLab, left) and four exemplary stimuli (right). (b) Trial structure of the more natural, free viewing condition (WildLab, left) and four exemplary stimuli (right)

screened and selected by criteria such as good visual acuity, straight camera angle and the presence of faces. As subsequent frames are highly similar, in a second screening, we checked the images again and excluded similar-looking pictures to ensure a high stimulus-appearance variability. Next, we manually marked all faces in each frame with rectangular bounding boxes. We concurrently classified human faces, human heads (facing away) and non-human faces, like mannequins or faces on advertisements. In the experiment, all stimuli were displayed with a magnification factor of 2.53, in order to be perceived at the same size as in the real world.

Due to limitations of the eye-tracking device, accurate calibration could only be ensured in the inner 60% of the width and height of the screen (with the participant sitting 80 cm away). Therefore, the full screen images had to be cropped. To do so, we defined 25 overlapping sections placed in a 5×5 grid over each image. For each image, one of the sections was chosen as a stimulus by means of the highest number of human faces present. When more than one cutout contained the same number of faces, the section with the largest face was chosen. The stimuli contained between one and seven human faces of different sizes and viewing angles. The size of the face annotation boxes ranged between $.08° \times .2°$ visual angle for the smallest and $5.2° \times 5.6°$ visual angle for the largest box. Although it would be interesting to classify all background objects fully, this was not a feasible option for this study. As the scenes are naturally crowded, an automatic and robust classification was not possible. As this study's question concerns the role of faces in comparison with other, various stimuli, we opted to classify all areas not manually tagged (as described before) as the category 'background'. For a more detailed description of the stimuli's properties, see Gert et al. (2020). This procedure resulted in two final sets of 171 images each. We presented each participant either the first or the second set, to minimize stimulus effects.

Ultimately, each stimulus was presented with a size of $30.5° \times 17.2°$ visual angle. As they were not presented full screen, the remainder of the screen was filled with a phase-scrambled version of the respective image to minimize the effects of the fixation's horizontal and vertical coordinate on the EEG signal (Dimigen et al., 2013).

2.5.2 | Experimental design

Each WildLab trial consisted of a fixation dot randomized between 1800 and 2200 ms in the screen centre, followed by 6000 ms of stimulus presentation and ended with a blank screen for a period randomized between 1600 and 2000 ms. The experiment contained 9 blocks of 19 trials each, with self-paced breaks after each block. During stimulation, the subjects performed a free viewing task, being allowed to freely explore the presented scene. Subjects were previously informed that they are also allowed to look at the phase-scrambled background but that it did not contain any information.

At the end of each block, before the break, subjects performed a self-controlled guided viewing task. They would see 51 successive markers, randomly presented on a 7×7 grid, starting and ending with a marker in the screen centre. Fixations of the respective marker were indicated by pressing the spacebar. These data are not analysed here.

14609568, 2022, 11, Downloaded from https://onlinelibrary.wiley.com/doi/10.1111/ejn.15824 by Universitatsbibliothek Stuttgart, Wiley Online Library on [27/05/2024]. See the Terms and Conditions (https://onlinelibrary.wiley.com/terms-and-conditions) on Wiley Online Library for rules of use; OA articles are governed by the applicable Creative Commons License

2.6 | Data analysis

All analyses were done in MATLAB (Release 2016b, The MathWorks, Inc., Natick, MA, USA) using the EEGLAB toolbox v. 14.1.1b (Delorme & Makeig, 2004). For integrating and synchronizing ET and EEG data, the EYE-EEG toolbox (http://www2.hu-berlin.de/eyetracking-eeg) was used (Dimigen et al., 2011).

2.7 | 2 × 2 statistical design

Following the literature, we are interested in the difference between processing faces and other objects. In addition, we introduce sequential effects, as we hypothesized that the previous fixation category will influence the processing of the current fixation. This effectively results in a 2 × 2 design with the factors Current and Previous, both with levels Face and Object.

2.8 | Eye tracking

In both experiments, fixations were detected by the Eye-Link system using the default Cognitive Configuration (SR Research, 2009, p. 91). The eye tracker uses an acceleration-based algorithm to determine saccades, and fixations are classified as the non-saccadic segments. That is, fixations are defined by being below a certain threshold of acceleration within the eye tracker's camera (velocity threshold: 30°/s, acceleration threshold: 8000°/s^2 and motion threshold: .15°) (Nyström & Holmqvist, 2010). Blink saccades, which were those spuriously detected due to blinks, were subsequently removed, by detecting whether a blink was enclosed between two saccades.

In the free viewing experiment, we identified the category of the currently fixated object and, to analyse sequential effects, of the previous fixation. We differentiated between fixations (i) on a human face, (ii) on a non-human face (mannequins, advertisements etc.), (iii) on a human head without a visible face, (iv) on the background of the scene or (v) outside the stimulus on the phase-scrambled border. Note that only fixations of type (i) are of interest and all other types were not directly investigated here. The mean number of fixations currently made on a face is 719.95 (range [504;1012]), whereas the average number of fixations made on the background is 1369.3 (range [832;1906]; for a detailed split into the 2 × 2 design, please see Table S1). Furthermore, we classified fixations whether they were on overlapping bounding boxes and whether consecutive fixations were within the same bounding box, that is, within the same face (μ = 233.5, range [106;452]).

Although we estimated fERPs for all previously mentioned conditions, we focus on the previously introduced 2 × 2 design. In addition to the main effects of previous and current fixation category and the interaction, we additionally investigated subsequent fixations on the same face (Figure 2).

2.9 | EEG

2.9.1 | Preprocessing

The eye-tracking data were imported and synchronized with the EEG with the help of the EYE-EEG toolbox (v0.8) for EEGLAB (Dimigen et al., 2011).

Then EEG data were downsampled to 512 Hz and highpass filtered at .1 Hz (EEGlab plugin firfilt with a cutoff frequency of −6 dB at .05 Hz, a hamming window and a length of 3381 points, Widmann et al., 2015).

Continuous data were visually inspected and artefactual sections were manually marked (muscle artefacts) and noisy channels removed (mean: 25.8, range: 19–34). Next, we used an independent component analysis (ICA; amica12, Palmer et al., 2012) to remove components with eye-muscle artefacts (Plöchl et al., 2012). Only for this step, the data were highpass filtered at 2 Hz to increase decomposition quality (Dimigen, 2020). The ICA weights were then re-applied on the downsampled and continuous data. The ICA components were visually inspected and muscle and eye movement components were removed from the continuous data causally filtered at 1 Hz based on their topography, spectrum and activation over time (mean: 22.41, range: 6–39). Investigating the timing of effects on the ERP filtering during preprocessing has to be considered. Specifically, commonly used symmetrical acausal filters utilize information from the past as well as from the future in the calculation of the electric potential at each point in time. That is, depending on the width of the filter, the filtered value at, for example, 100 ms after fixation onset is influenced by the earlier data, for example, at fixation onset, and by later data, for example, 170 ms. In contrast, causal filters utilize only information from the past, meaning it prevents smearing back in time (Rousselet, 2012) and, for us, the exact onset of an event is of stronger interest than the offset. In our case, a causal filter results in an influence from earlier points in time; for example, the P100 is influenced by activity from fixation onset, but not from later points in time, for example, at 170 ms. That is, using a causal filter, a potential effect at 170 ms does not influence the data at 100 ms after fixation onset. Therefore, for the investigation of an early effect, using causal filters

14609568, 2022, 11, Downloaded from https://onlinelibrary.wiley.com/doi/10.1111/ejn.15824 by Universitatsbibliothek Stuttgart, Wiley Online Library on [27/05/2024]. See the Terms and Conditions (https://onlinelibrary.wiley.com/terms-and-conditions) on Wiley Online Library for rules of use; OA articles are governed by the applicable Creative Commons License

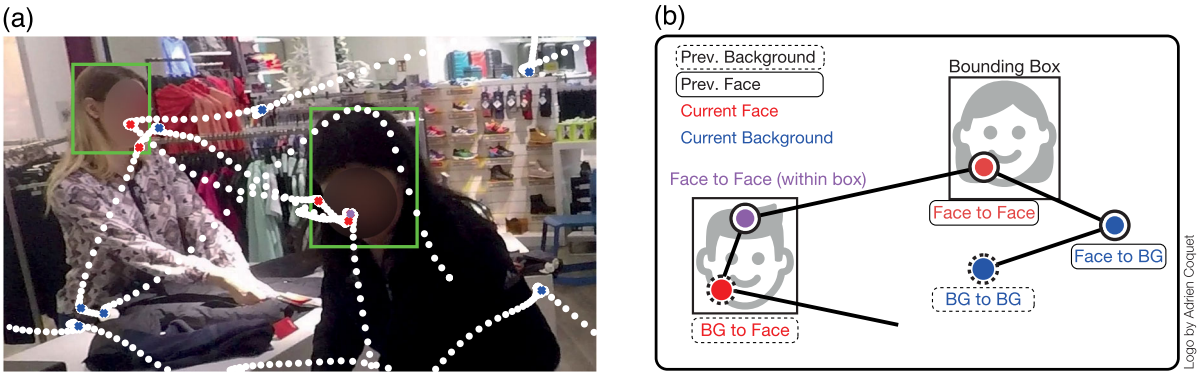

FIGURE 2 Exemplary eye-tracking data of one trial and schematic visualization of the 2 × 2 categorization. (a) Eye-tracking data of one subject. White dots represent the single samples, whereas the crosses represent the fixations as detected by the eye tracker. For visualization purposes, the faces are overlaid with their respective bounding boxes. (b) Fixations were categorized by their origin and their current placement. We distinguish between fixations made on the background (blue) or a face (red). For face to face fixations, we additionally specify whether they are the first fixation on a face or a refixation within the same bounding box (within face fixations, purple).

during preprocessing is the method of choice. This is especially critical in the case of pre-fixation onset events, where we need to be sure that they occurred before the fixation and are not a smear-back due to an acausal filter. Furthermore, a highpass with a passband edge of 1 Hz (−6 db cutoff at .5 Hz) was chosen, as the deconvolution kernel was of length 2 s, and we wanted to preclude potential problems with low frequencies. In other words, the filter we chose minimized this interaction between low frequencies and the deconvolution. Data were re-referenced to average reference and removed channels were interpolated using spherical interpolation.

Because we need to correct for overlapping activity and eye-tracking parameters, we used a regression-based approach implemented in the unfold toolbox (Ehinger & Dimigen, 2019). A linear model including the factors Previous and Current (each consisting of the levels Background, HumanFace and Other), the factor Samebox (if multiple fixations were made within the same face) and an interaction term was defined for the fERP. Furthermore, spline regression was used to model non-linear effects of horizontal and vertical fixation position and saccade amplitude on the EEG. Additionally, the stimulus onset-driven ERP was modelled to correct for the overlap between the stimulus onset and the first fixation. This time expansion and thus overlap correction were applied between −500 and 1000 ms relative to fixation onset.

The data were modelled with the following Wilkinson notation (Wilkinson & Rogers, 1973) in the unfold toolbox by

$$\begin{aligned}\text{Fixation ERP} \sim 1 &+ \text{currently fixating a face}\\ &+ \text{previously fixating a face}\\ &+ \text{currentlyOnFace} : \text{previouslyOnFace}\\ &+ \text{within face fixation}\\ &+ \text{spline}(\text{fixation position x}, 5)\\ &+ \text{spline}(\text{fixation position y}, 5)\\ &+ \text{spline}(\text{saccade amplitude}, 5)\end{aligned}$$

$$\text{Stimulus ERP} \sim 1$$

We used the same overlap correction for the ClassicLab condition, even though we expected no overlapping activity between trials. However, participants did make some rare eye movements in the 300 ms stimulus presentation, which might influence the ERP (Dimigen & Ehinger, 2021); on the other hand, we keep comparability between conditions maximal by using the same analysis algorithms.

The ClassicLab condition data were modelled with the following Wilkinson notation:

$$\begin{aligned}\text{Fixation ERP} \sim 1 &+ \text{spline}(\text{fixation position x}, 5)\\ &+ \text{spline}(\text{fixation position y}, 5)\\ &+ \text{spline}(\text{saccade amplitude}, 5)\end{aligned}$$

$$\begin{aligned}\text{Stimulus ERP} \sim 1 &+ \text{currently a face} + \text{previously a face}\\ &+ \text{currently a face:previously a face}\end{aligned}$$

For a visualization of the effects of the deconvolution on the (f)ERPs, see Figure S2.

14609568, 2022, 11, Downloaded from https://onlinelibrary.wiley.com/doi/10.1111/ejn.15824 by Universitatsbibliothek Stuttgart, Wiley Online Library on [27/05/2024]. See the Terms and Conditions (https://onlinelibrary.wiley.com/terms-and-conditions) on Wiley Online Library for rules of use; OA articles are governed by the applicable Creative Commons License

2.10 | ERP analysis

2.10.1 | N170 analysis

The epoched, deconvolved ERP estimates were averaged over the occipital electrodes P7, PO7, P8 and PO8 according to Rossion and Jacques (2008). The amplitude of the N170 was determined as the minimum in the time range of 130 to 200 ms after fixation or stimulus onset according to Rossion and Jacques (2008), whereas the P100 was defined as the maximum between 80 and 130 ms after the event of interest. After observing that some subjects had a P100 peak later than our initial prespecified time limit of 130 ms, we extended the time limit to 150 ms for all subjects. Additionally, in the lab condition, the N170 peaked earlier. Therefore, the time limits for the N170 were adjusted to 120 to 200 ms. For details on the mean and 95% confidence interval (CI) of these values, see Table S2.

2.10.2 | Mass univariate

Besides only performing the classic N170 analysis, we used the mass univariate approach to analyse the deconvolved ERPs for all electrodes and time points. Statistical testing was done using a one-sided *t* test of parameter estimates at each time point with an alpha level of .05. The multiple comparison problem was corrected using a cluster-based permutation test with threshold-free cluster enhancement (TFCE) with 10.000 permutations. For each permutation, we randomly flipped the signs of each subject's parameter estimate, calculated the *t* values and enhanced them using TFCE, generating an empirical H0 distribution of TFCE enhanced *t* values. The maximum over the time range of −500 to 1000 ms was used to construct an H0 TFCE-value distribution, against which the actual TFCE enhanced *t* values were compared. We considered *t* values above the 95th percentile of this distribution to be significant.

2.10.3 | Correlation and effect size

The correlation between the N170 amplitude from ClassicLab and WildLab was calculated using the skipped Pearson correlation implemented in the robust correlation toolbox (Pernet et al., 2013). To minimize the effect of signal differences in previous time points, the peak-to-peak amplitude between the P100 and N170 was calculated (Handy, 2005). We then subtracted the object trials' peak-to-peak amplitude from the face trials' peak-to-peak amplitude, resulting in a difference value for face processing for each subject in both the ClassicLab and WildLab conditions; $peak\text{-}to\text{-}peak\ effect = (amplitude_{P100} - amplitude_{N170})_{Face\ trials} - (amplitude_{P100} - amplitude_{N170})_{Non\text{-}face\ trials}$. Seeing our high correlation value, we were interested whether this correlation value is compatible with a perfect correlation and calculated the noise ceiling of an assumed perfect correlation, given the between-subject (σ over subjectwise means, ClassicLab: 1.6, WildLab: 1.0) and within-subject variability (mean of subjectwise standard errors, ClassicLab: .73, WildLab: .55). To simulate the between-subject variabilities, we sampled 20 new values from a normal distribution and scaled them each once by the condition-wise between-subject variability. This led to 2×20 values with a correlation of 1 (i.e., perfect). Because we cannot perfectly measure these data points, we added the within-subject sampling variability: For each subject and condition separately, we drew a random number from a normal distribution, scaled it by the respective within-subject variabilities and added it. We repeated the procedure 1000 times, with each repetition resulting in a 2×20 matrix. For these randomly sampled results, we calculated the Pearson correlation coefficient. The resulting distribution of Pearson correlations can be used as a parametric estimate of the H0 distribution taking measurement error into account. The median of this distribution is .8, whereas our observed correlation value is .78.

In order to calculate whether the between-subject variance in the WildLab condition was lower than in the ClassicLab condition, we bootstrapped the individual experiment's standard deviations. This procedure was done 10.000 times with all subjects detected as not being outliers in the robust correlation (see Figure 3c). Furthermore, we calculated the bootstrapped 95% CI (10.000 repetitions, BCa) for the difference between the Cohen's d_z of ClassicLab and WildLab to estimate the difference in effect size with $d_z = \mu(\text{peak-to-peak}_{Face} - \text{peak-to-peak}_{Object}) / \sigma\left(\text{peak-to-peak}_{Face} - \text{peak-to-peak}_{Object}\right)$.

3 | RESULTS

3.1 | The free viewing paradigm replicates classic face processing ERPs, while reducing the cross-participant variance

The ClassicLab condition contrasts photographs of isolated faces and objects. We observe well-known signatures of face processing. These are predominantly visible as a negative ERP peak at around 170 ms (Figure 3a), with face trials showing a more negative deflection than trials on objects at individual N170 peaks (Faces: mean

14609568, 2022, 11, Downloaded from https://onlinelibrary.wiley.com/doi/10.1111/ejn.15824 by Universitatsbibliothek Stuttgart, Wiley Online Library on [27/05/2024]. See the Terms and Conditions (https://onlinelibrary.wiley.com/terms-and-conditions) on Wiley Online Library for rules of use; OA articles are governed by the applicable Creative Commons License

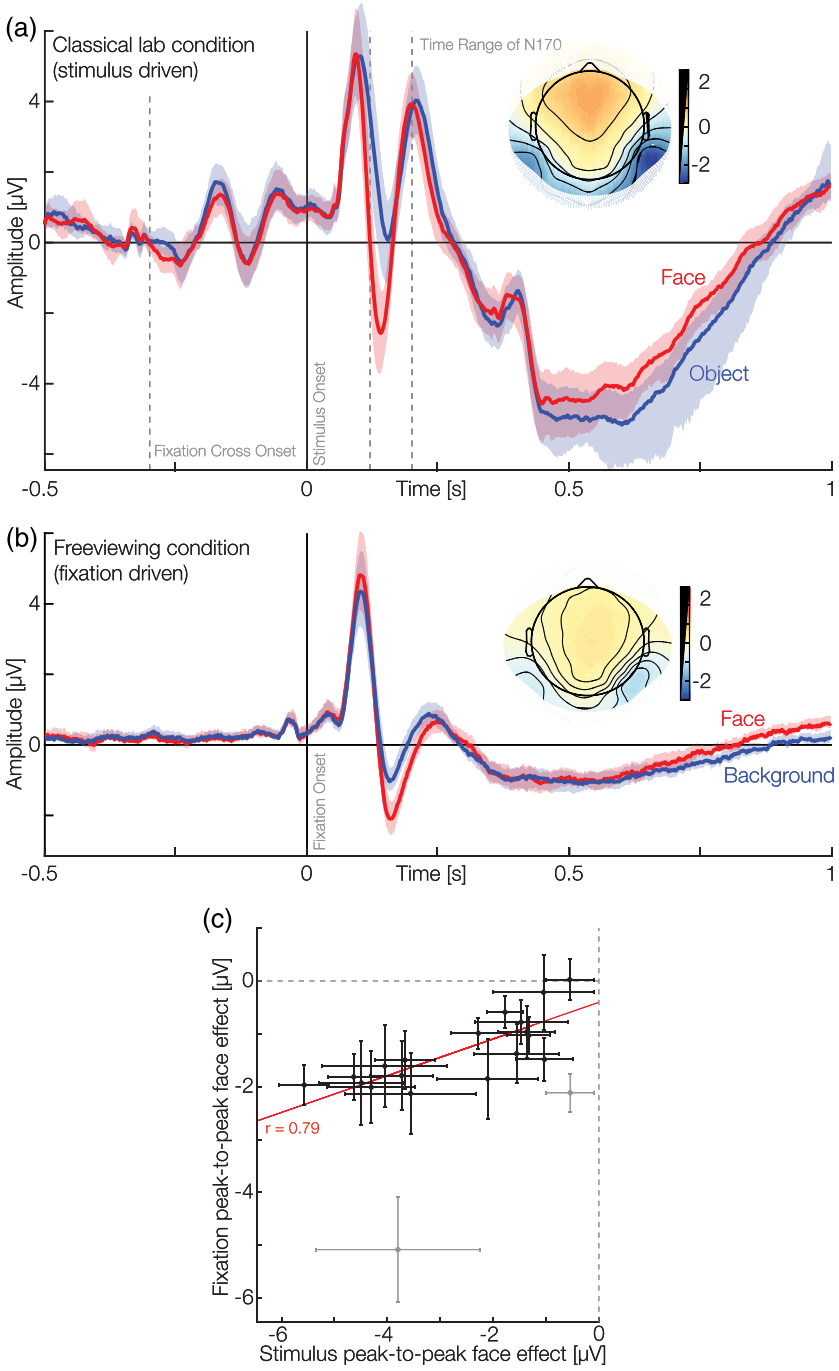

FIGURE 3 Event-related potentials (ERPs) of the ClassicLab and WildLab conditions (average over P7/8 and PO7/8) and their correlation displayed with average reference. (a) Stimulus-driven ERP of the ClassicLab condition. With our experiment, we can reproduce previous findings of the N170 being larger when faces are presented. Please note that the deflections in the baseline period stem from a non-jittered fixation cross presentation. This issue is not present in the WildLab condition, as the stimulus onset was jittered instead of fixed. The shaded area shows the 95% bootstrapped confidence interval (CI) of the mean over participants for each condition individually (10.000 iterations, BCa). The topographic plot visualizes the average activity of the N170 time range for all electrodes. (b) Fixation-driven fERP of the WildLab condition. Here, we can see that fixations on a face produce a more negative N170 than those on the background. Additionally, the topography shows a generally weaker activation but the same parieto-occipital pattern of stronger right lateralization. (c) Correlation of the peak-to-peak effects. The peak-to-peak differences (amplitudes of P100–N170, face trials–non-face trials) in the passive and active conditions correlate (r = .79; bars represent the standard error). Grey data points were automatically excluded by the robust statistics toolbox. Please note that all data shown in this plot are corrected for overlap and eye-movement-dependent effects.

individual maximum of −3.5 μV [95% CI: −4.6;−2.3 μV], Objects: −.8 μV [−2.1;.3], difference: −2.7 μV [−3.5;−2.1]; further comparisons in Table S2). We do not see a difference in the P100 peak amplitudes (Faces: 6.0 μV [95% CI: 4.7;7.3], Objects: 6.2 μV [4.9;7.6], difference: −.2 μV [−.5;.1]). These results qualitatively agree with early reports of the N170.

Next, we investigate fixation-related ERPs in the WildLab condition on natural scenes. Collapsing over sequential effects, and controlling for temporal overlap and the effects of eye movements, we observe that the fixation-induced ERP (fERP) is modulated by fixations on faces. In particular, the N170 is more negative for fixations on a face than those on the background (Figure 3b, Faces: −2.5 μV [95% CI: −2.9;−2.2], Background: −1.4 μV [−1.7;−1.1], difference: −1.1 μV [−1.5;−.9]). At the same time, the more natural paradigm leads to a stronger P100 when a face is fixated (Faces: 5.2 μV [95% CI: 4.3;6.3], Background: 4.8 μV [3.9;5.8], difference: .4 μV [.3;.7]; further comparisons in Table S2). In summary, these findings replicate previous passive presentation experiments in a more natural setting but

14609568, 2022, 11, Downloaded from https://onlinelibrary.wiley.com/doi/10.1111/ejn.15824 by Universitatsbibliothek Stuttgart, Wiley Online Library on [27/05/2024]. See the Terms and Conditions (https://onlinelibrary.wiley.com/terms-and-conditions) on Wiley Online Library for rules of use; OA articles are governed by the applicable Creative Commons License

also provide evidence that, under such natural viewing conditions, additional effects occur at earlier processing stages.

In addition to the presence of face-related N170 effects in both paradigms, we perform a more stringent test of the statement that the same face-related brain processes are at play and correlate the effect sizes in both conditions across participants (Figure 3c). Indeed, a robust skipped Pearson correlation of the peak-to-peak N170 effect shows a strong correlation ($r = .79$ [.63;.92]). Assuming a perfect correlation and taking into account the within- and between-subject noise estimates (noise ceiling, see Section 2), this value is within the upper bound of observable correlations. These results show that participants with a stronger N170 effect in the ClassicLab condition also show a stronger N170 effect in the more naturalistic WildLab condition, meaning that individual differences generalize to more ecologically valid setups. Interestingly, we do not only observe smaller between-condition differences but also a lower between-subject variance in the WildLab condition than in the ClassicLab condition (with a standard deviation of .6 μV [95% CI: .5;.9] and 1.5 μV [1.3;2.0], respectively, difference [.5;1.2]). Investigating the effect sizes between the experiments leads to non-significant differences (Cohen's d of ClassicLab [95% CI: 1.3;2.2], WildLab [1.3;3.2], difference [−1.5;.2]). This result suggests that the absolute size of the variance in more natural settings is smaller, although we cannot make a statement about differences in effect size. Future studies are needed to investigate these effects further.

3.2 | Unrestrained spatiotemporal analyses reveal further effects of face processing across subsequent fixations

Having verified our experimental and analysis approach, we expand our analyses beyond the commonly used, yet restricted set of electrodes and time windows. This allows us to analyse the complete temporal dynamics of face processing across all electrodes. In addition to the object category viewed at the current fixation (face vs. background), we model whether a fixation was previously on a face. Including this sequential predictor in the model further allows us to investigate the interactions between the current and the previous fixation category. Finally, we include the influence of gaze shifts within a single face and between different faces (Figure 2b).

Based on our analyses of the model, we observe a significant difference (cluster permutation test with TFCE-corrected $\alpha = .05$) in the main effect for the current fixation type, face versus background, beyond the commonly investigated effect time and location. This difference is likely driven by two clusters from 74 to 242 ms, in frontal parieto-occipital and occipital electrodes (Figure 4a, thick black lines and thick black circles). Temporally, two components can be distinguished: An early positive P100 at occipital electrodes with a topography implicating processing in the early visual regions (peaking at 1.24 μV) and a later bilateral N170 effect, dominant at parieto-occipital electrodes (peaking at −1.65 μV). Interpreting the topography during the time point, both clusters are accompanied by what seems to be their respective frontal equivalent dipole counterpart, which for the N170 is often termed the VPP (Joyce & Rossion, 2005; for a review on the VPP, also concerning the role of eye movements, see Jeffreys, 1996). Strong statements about our signal's origin cannot be made, as neither source localization was performed nor structural data for our participants were available, but it is a reasonable conclusion to us.

These results support our findings on the N170 discussed before and further demonstrate that voluntary fixations on natural faces lead to earlier differences, including the timeframe of the P100, which has been extensively discussed in the literature (Herrmann et al., 2005; Liu et al., 2002).

In addition to analyses of the main effects of face processing based on the category of the *currently* fixated object, we next analyse the main effect of the *previous* fixation. That is, we investigate the difference between fixations coming from the background versus those coming from a face, regardless of the currently fixated category (the classical ERP plot can be found in Figure S1). This reveals significant effects that originate from clusters in frontal and parieto-occipital electrodes (Figure 4b). Notably, the cluster starts about 50 ms before fixation onset and extends up to 256 ms after fixation onset. The cluster topography implies the same source configuration as the N170, but as an inverted effect: more positive in parieto-occipital and more negative in frontal electrodes (peaks at 1.7 and −.62 μV, respectively). Together with the main effect observed for the current fixated category, this means that not only is the N170 less strong when previously fixations were on a face but also this modulatory effect appears already before the new fixation started. A shorter second cluster shows effects between 469 and 510 ms (peak at −.43 μV) in a small set of electrodes. To conclude, when performing a saccade coming from a face, the EEG activity elicited by the current fixation will be more positive in typical N170 sources, even before the current fixation onset, clearly indicating sequential effects across subsequent fixations.

Having investigated the two main effects, the category of the current and previously fixated objects, we examine

14609568, 2022, 11, Downloaded from https://onlinelibrary.wiley.com/doi/10.1111/ejn.15824 by Universitatsbibliothek Stuttgart, Wiley Online Library on [27/05/2024]. See the Terms and Conditions (https://onlinelibrary.wiley.com/terms-and-conditions) on Wiley Online Library for rules of use; OA articles are governed by the applicable Creative Commons License

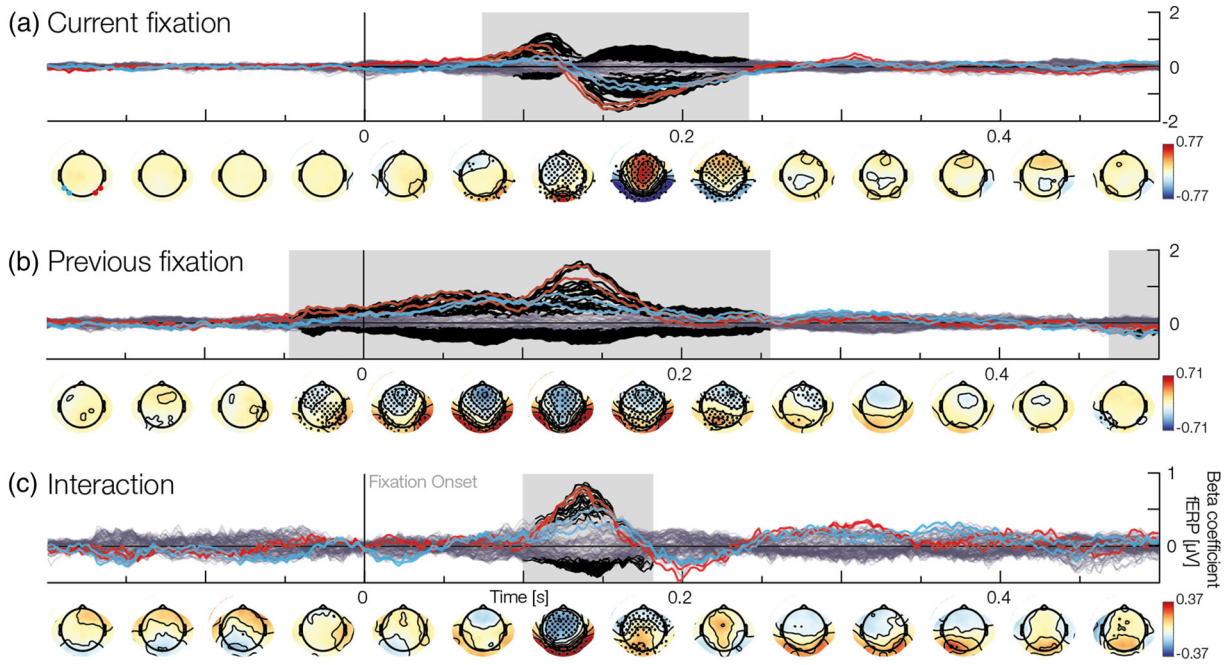

FIGURE 4 Model results of the WildLab condition (red lines indicate the beta for the classic N170 electrodes; light grey lines are the betas of all other electrodes). (a) Effect of the current fixation. When currently fixating a face, the amplitude will be stronger in the P100 and N170 range (black lines and black dots). Channels marked in red are P8/PO8 and those marked in blue are P7/PO7. Shaded grey areas denote time ranges of statistically significant clusters. (b) Effect of the previous fixation. When saccading from a face, the amplitude will be more positive than the intercept in parieto-occipital and more negative in fronto-central electrodes. This effect is already present before fixation onset until after the N170. (c) Interaction of the current and previous fixation. When participants saccade between two faces, the event-related potential (ERP) will be significantly decreased during the N170. All effects here were modelled using effects coding (−.5 for background, .5 for faces).

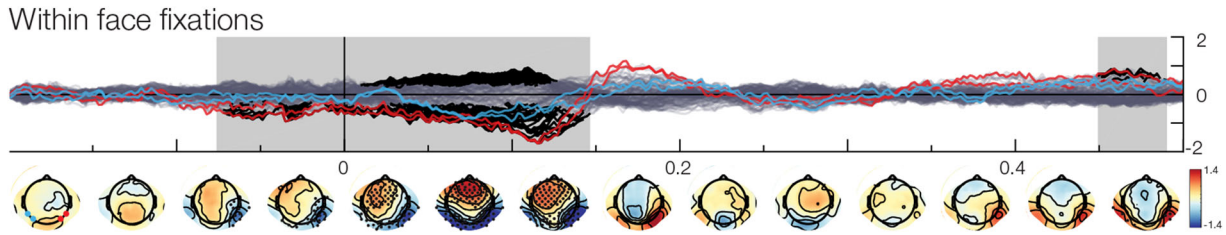

FIGURE 5 Results of saccading within the same face. When consecutive fixations are made within the same face, the activation will be weaker even before fixation onset starting in electrodes normally associated with the N170. This indicates an adaptation effect up until the N170. Please note that even though the betas show an opposite behaviour to Figure 4, the effect is the same, due to the coding in our model. This interaction is coded with 0 for non-faces and 1 for faces when saccading within the same bounding boxes.

them in light of their interaction. Testing the interaction term reveals a significant cluster with positive and negative activations from 100 to 182 ms (Figure 4c). The negative betas are strong in frontal electrodes with a peak of −.43 μV, whereas the positive betas, peaking with .88 μV, are located at parieto-occipital electrodes. Combining this with the two main effects of previous and current fixation, this result implies that the N170 has a smaller amplitude (i.e., is more positive) if a participant saccades between two faces. This effect can be understood in terms of neural adaptation effects. Notably, the early part of the main effect of the previous fixation shows no co-occurring interaction. Thus, the early part of the main effect of previously fixating a face seems to resemble a reactivation of the previous fixation type, and the potential adaptation effect is therefore limited to the neuronal substrate activated relatively late in the process.

Although our previous analyses focus on fixations between the background of a scene and faces, or across separate faces, some fixation sequences appear within the same face (Figure 5). Analysing these data, we observe a significant interaction including a first cluster located

14609568, 2022, 11, Downloaded from https://onlinelibrary.wiley.com/doi/10.1111/ejn.15824 by Universitatsbibliothek Stuttgart, Wiley Online Library on [27/05/2024]. See the Terms and Conditions (https://onlinelibrary.wiley.com/terms-and-conditions) on Wiley Online Library for rules of use; OA articles are governed by the applicable Creative Commons License

parieto-occipitally, starting in electrodes on the right hemisphere at around −75 ms and spreading bilaterally over time until 146 ms, peaking at −3.41 μV (frontal electrodes peak at 1.88 μV). A second weak and short cluster around 475 ms is located in the right occipito-temporal electrodes starting at 449 until 490 ms, but due to the distance to the fixation event, this remains difficult to interpret. In summary, performing two consecutive fixations on the same face will lead to a weakened ERP signal between the saccade onset and the P100, indicating a preview and adaptation effect.

4 | DISCUSSION

4.1 | Reproducing and extending the classic observations

The main goal of this study is the validation and extension of classic experimental results under more naturalistic experimental conditions. Although previous studies used naturalistic setups, they either employed everyday stimulus material but lacked eye movements (Cauchoix et al., 2014; Johnston et al., 2015) or allowed for eye movements but used artificial stimulus material (Auerbach-Asch et al., 2020; de Lissa et al., 2019; Soto et al., 2018). These studies advanced face perception research but lacked the crucial combination of embodiment and natural stimulus material. Previous literature showed that the neural correlates of perception differ between passive and active perception (Auerbach-Asch et al., 2020; Ehinger et al., 2014; Kaunitz et al., 2014) and that naturalistic stimuli will lead to different activation from artificial ones (Hasson et al., 2004; Johnston et al., 2015). As the combination of these two aspects is what we encounter in our everyday life, it is necessary to combine them to obtain the full picture of naturalistic face perception. Not only are we able to confirm results classically reported in passive perception experiments (Rossion & Jacques, 2008), but we also replicate the findings of one of the first studies combining free viewing and face perception (Auerbach-Asch et al., 2020). In line with this previous paper, we find an enhanced N170 when looking at faces in contrast to other objects. Yet, with our approach of using naturalistic scenes, we could demonstrate that more naturalistic face processing will lead to earlier effects than reported in this earlier study, including time points classically defined as the P100, and extend beyond parieto-occipital electrodes, throughout the whole scalp. This indicates extensive processing including a strong activation of the underlying neuronal sources, which could be the posterior superior temporal sulcus and the fusiform face area (Sadeh et al., 2010; see Weiner & Grill-Spector, 2013, for a review). However, our results contrast those by Soto et al. (2018). In his study, subjects freely viewed a real-world stimulus display containing pictures of cutout faces or objects. This omits the role of embedding stimuli in their natural environment. A fixation's onset was manually defined as the first sample moving onto a face irrespective of the eye's current speed. Therefore, the measured activity might have included saccadic activation. In addition, Soto et al. did not control for eye-movement-related parameters or overlap. Thus, the difference to our study might be due to the difference in defining the fixation onset and their lack of statistical control for eye movement parameters. To conclude, here, we replicate the classic findings in more natural settings and further extend these observations to larger time ranges, than reported in a previous free viewing paradigm, including the early parts of the visual response.

4.2 | Similar processes in classic and the more naturalistic conditions

Whether our fixation and more traditional stimulus-evoked responses describe the same processes is an important question. Although previous studies have shown that face processing-related eye movements generalize from lab-based settings to mobile recordings (Peterson et al., 2016), this generalization is especially debated for the P100 and the lambda response, but also the N170 and the N1 of the lambda complex (Kazai & Yagi, 2003). Here, we focused on the correlates of face processing, as described by the difference in the P100/N170 peak-to-peak amplitude. Still, our study adds to this discussion, as we found a high correlation of .78 between eye movement N1 and traditional N170, well within the noise ceiling. It could be argued that the N170 face effects are, actually, uncorrelated, and we observe the correlation purely due to non-specific between-subject effects like individual anatomy, skull thickness or conductivity (Antonakakis et al., 2020). We think that this is not the case here: If the face-selective effect would not exist in, for example, the free viewing condition, we would expect a correlation around zero, which we think is incompatible with our observed correlation coefficient. Nevertheless, could the correlation coefficient be overestimated, given that, for example, due to skull thickness, responses in some subjects are generally larger than in others, irrespective of stimulus? Again, we do not think so, as in our case, we use the subtraction method, where we control for condition-independent peak-to-peak amplitude, by using the difference between face and non-face ERPs.

14609568, 2022, 11, Downloaded from https://onlinelibrary.wiley.com/doi/10.1111/ejn.15824 by Universitatsbibliothek Stuttgart, Wiley Online Library on [27/05/2024]. See the Terms and Conditions (https://onlinelibrary.wiley.com/terms-and-conditions) on Wiley Online Library for rules of use; OA articles are governed by the applicable Creative Commons License

Thus, any observed effect correlation is not a pure amplitude correlation but a correlation of the effects. This is not to say that there is no variability in the size of the peak-to-peak face effect between subjects; on the contrary, whatever the source of this variability, it seems to be preserved from lab to free viewing conditions.

As a disclaimer to our correlation analysis, we want to note that correlations computed on a small number of participants, for example, less than 100, have typically low power (Schönbrodt & Perugini, 2013; Yarkoni, 2019). However, here, we are investigating within-subject correlations, which have typically higher power than between-subject correlations. Thus, the high correlation values and very similar effect topographies implicate the same face processing in passive and active contexts. This leads us to believe that the N170 and general lab-based face processing results generalize to more naturalistic setups, indicating that the found effect truly holds in everyday vision.

An important property of our study is that we investigated classic and naturalistic experimental settings within the same subjects. Besides the robust correlation of the N170 amplitude across the traditional and naturalistic experimental conditions, we found that the between-subject variance in the naturalistic condition is smaller than in the classic setup. This came as a surprise, as the naturalistic setup contains more sources of variation, for example, different gaze trajectories by different subjects. Thus, it appears that the difference in visual processing of faces versus non-faces is more comparable across subjects under naturalistic conditions. As a note of caution, with the currently available data, we cannot make a definite statement with regard to the effect size. Future studies with more subjects might allow investigating the effect of ecological validity on inter-subject consistency. A highly speculative interpretation of this observation is that evolutionary constraints act under naturalistic conditions. Although processing an isolated image of a flashed face allows us to measure isolated effects during face processing, it has less direct consequences for evolutionary success. However, the active fixation and visual processing of faces under naturalistic viewing conditions are arguably more directly related to relevant social interactions. That is, due to evolutionary constraints, visual processing might be more consistent between humans under relevant naturalistic conditions as compared with artificial situations that the experimental subjects did not encounter before. If this speculative interpretation holds up in other studies as well, it would be a strong argument to investigate sensory processing under naturalistic conditions in general.

4.3 | Sequential effects during trajectories of fixation points

Our free viewing paradigm allows us a deeper insight into brain function, by analysing sequential effects of fixation history. Our results show a positive shift in the ERP beginning before the current fixation for fixations originating from a face being more positive. This effect cannot be explained by a parafoveal preview (Buonocore et al., 2020), as it is only dependent on the category of the previous fixation, and not the current one, and no interaction between the two was found in the early period of time (only during the N170 time window). This effect might be attributed to some kind of neuronal fatigue or a special type of adaptation effect. Note that this is not a classic adaptation or classic repetition suppression effect; we only have stimulus specificity of the previous fixation target, but not of the current one. Thus, one possible hypothesis is that after processing a face during the previous fixation, the face processing system might exhibit a general reduction of activity, irrespective of the current stimulus. This depletion might reduce the activity of the stimulus-type unspecific part of the fusiform sources (fusiform sources as a general term to the areas that give rise to the N170 topography). This explanation would require a special interaction of the face-specific fusiform areas with the unspecific fusiform areas, to explain that the effect is specific to face perception in the previous fixation, but unspecific to the current one. Alternatively, but more speculatively, it might be the case that at (and before) each fixation, we activate the face system leading to a 'default' face-selective N170, irrespective of whether a face will be fixated or not. Combined with repetition suppression (e.g., Summerfield et al., 2011) following a previous face fixation, this would explain a general reduction of activity throughout (and before) the fixation. Although previous studies reported (Auerbach-Asch et al., 2020; Buonocore et al., 2020) a reduction of amplitude after face perception, these findings report repetition effects (face to face saccades) and not the effect reported here, which is independent of the currently fixated category. Notably, the fERP in our study is changing earlier than previously reported (Jacques et al., 2007; Kovács et al., 2006; Schweinberger & Neumann, 2016), which find adaptation effects starting during the period of the N170. It has to be noted that there classic adaptation paradigms were used like the repetition of a certain category or a specific identity. This is not the case in our paradigm, as participants freely chose where to look next.

In the cases when a saccade was made within a face, we found an ERP difference to between-face fixations. This difference in activity is in line with previous research (Auerbach-Asch et al., 2020) and could be due

14609568, 2022, 11, Downloaded from https://onlinelibrary.wiley.com/doi/10.1111/ejn.15824 by Universitatsbibliothek Stuttgart, Wiley Online Library on [27/05/2024]. See the Terms and Conditions (https://onlinelibrary.wiley.com/terms-and-conditions) on Wiley Online Library for rules of use; OA articles are governed by the applicable Creative Commons License

to adaptation effects to the specifics of the face, extending over and beyond the interaction of the previous and current fixation previously described. Our finding contrasts those of Amihai et al. (2011), who found no specific effect of identity repetition in a passive viewing paradigm. This dissimilarity might be attributed to the differences in the timeline of each trial, with trial durations being either drastically shorter or longer than the fixations measured in our experiment. Interestingly, our finding extends to time points even before the onset of the fixation, potentially resulting from a type of within-face preview effect. Concerning this hypothesis, our results contrast those of previous studies that found no pre-fixation differences for congruent versus incongruent peripheral previews (Buonocore et al., 2020; de Lissa et al., 2019; Huber-Huber et al., 2019). In our case, the participants were already looking at the face while refixating it, which might introduce an even stronger effect that is specific to free viewing paradigms. It is, therefore, a necessity to understand natural face processing in light of its recent history.

4.4 | A new methodology that allows for this type of analysis

In this study, we model both temporal overlap of neural processes in time and non-linear influences of eye movement parameters (e.g., saccade amplitude or saccade position), which can lead to systematic differences between conditions (Dimigen et al., 2011; Dimigen & Ehinger, 2021; Nikolaev et al., 2016). Such regression-based deconvolution models are increasingly becoming popular (e.g., Cornelissen et al., 2019; Dandekar et al., 2012; Dimigen & Ehinger, 2021; Kristensen et al., 2017; Smith & Kutas, 2015). The adequacy and necessity of our deconvolution approach can be seen in Figures S2 and S3, where we contrast it with a non-deconvolution analysis. Without overlap correction, we see additional large differences for face versus background already in the pre-fixation period and after 300 ms. They can be attributed to two different overlap effects: The first effect is due to biased overlap with the stimulus response. The first fixations after stimulus onset are predominantly made on faces (nearly 70%, Cerf et al., 2009; Gert et al., 2020; Hernández-García et al., 2020). Thus, without overlap correction, the fERPs of faces will be much more influenced by the stimulus ERP than background fixations leading to the observed bias. The second overlap effect is likely due to subsequent fixations. Fixation durations between faces and background fixation differed systematically, explaining this overlap effect (see Figure S4). Besides previous simulation work, our results leave us confident that applying deconvolution and non-linear coefficient modelling is the right tool to analyse eye-movement-related potentials.

4.5 | Limitations of the present study

This study explores a new paradigm and naturally comes with limitations and unexplored questions. These questions pertain to the stimulus material used and eye movements as quasi-experiments.

In our study, we make use of a set of ecologically valid stimuli without photographer bias (Gert et al., 2020; Tatler, 2007). This has advantages and disadvantages. On one hand, the stimulus material is less well controlled; for example, faces are viewed in many different sizes and from many different angles. That is, there might be statistical differences between faces and the background in features like contrast, colour, orientation or luminance and in the variation of such properties. Previous studies have highlighted the influence of such features as driving forces behind effects on the P100 (Ganis et al., 2012; Rossion & Caharel, 2011; Rousselet et al., 2008). Considering these possible differences, the faces presented here can be inherently more similar to each other than other objects (Thierry et al., 2007). The issue of between-face similarity has been extensively discussed and was refuted in light of the N170 (Rossion & Jacques, 2008). These differences can be seen as a limitation; that is, the observed effects of viewing faces on the P100 and N170 are qualified in comparison with the differing background. That is, in the present study, a statement of face-selective effects has to be interpreted in comparison with the naturally occurring background.

These limitations discussed above can also be seen as a feature: If findings should generalize to other tasks and contexts, then they should be tested with a variable stimulus set. Although there has been a move towards more ecologically valid stimulus materials in face processing (e.g., Kamienkowski et al., 2018; Retter & Rossion, 2016), the typical cognitive neuroscience stimulus is quite specific; this lack of stimulus variability has recently been coined as the 'generalizability crisis' (Yarkoni, 2019). Thus consequently, our statistical method should reflect the increased variability by addressing both between-subject and between-item effects. Unfortunately, it is currently computationally infeasible to adequately model this in combination with overlap correction (as argued by Cornelissen et al., 2019; but see Ehinger, 2019, for a counterexample). In addition, we argue that the very nature of natural stimulation necessarily implies a mixture of various signal sources, some of which can be

14609568, 2022, 11, Downloaded from https://onlinelibrary.wiley.com/doi/10.1111/ejn.15824 by Universitatsbibliothek Stuttgart, Wiley Online Library on [27/05/2024]. See the Terms and Conditions (https://onlinelibrary.wiley.com/terms-and-conditions) on Wiley Online Library for rules of use; OA articles are governed by the applicable Creative Commons License

artificial when experiments become more naturalistic and motion is allowed (Oliveira et al., 2016), but most of them are likely being used by the brain to extract meaning from the world.

In the present study, we chose to compare these findings with those from a common passive perception task on strongly controlled face stimuli (e.g., controlling for size and using proper illumination). Although these two paradigms differ in terms of low-level features, this choice was deliberate as the two stimulus sets reflect (a) the most common experimental paradigm for face selectivity (well controlled) and (b) the currently explored counterpart, which likely resembles the most naturalistic condition that can be measured in a lab setting. Filling the space in between these two extremes, future studies could include a passive perception task with faces taken from the scene images or a free viewing task with the controlled stimuli. Still, our finding of a strong correlation between the two settings underlines the success of the naturalistic paradigm. Further, it should be noted that reduced control is an unpreventable result of studying vision in a more natural setting. Voluntary eye movements are a quasi-experimental setting that precludes randomization. Thus, causal statements like 'fixating a face causes a larger N170' are more difficult to prove than in a classic experiment. Ultimately, we cannot completely exclude the possibility that an N170 evoked by eye movements is the result of a mediation effect induced by contrast or luminance differences between fixation positions, as we cannot distinguish these factors with our dataset. On the other hand, the high diversity in our stimulus material in terms of low-level features has advantages as well. We present faces in a wide variety of viewing angles, distances and, therefore, size, and lighting conditions. This natural variation leads to a lower within face similarity and thereby weakening the face similarity's influence on the N170 amplitude. Further, it allows statements like 'fixating a face under naturalistic conditions causes a larger N170 than fixating the background under these conditions'.

Summing up, here, we advanced neuroscientific studies on face processing in multiple ways. We provide a naturalistic study setup, using natural scenes and allowing for eye movements, and combine this with an analysis pipeline that overcomes the technical challenges that are posed by this more natural setup. We reproduce previous findings from passive viewing and more controlled stimulus materials and show that the old and new effects closely relate to each other. Our findings also show that with a free viewing paradigm, we can find previously unknown effects of eye movement history on ongoing face processing, opening new avenues of research for exploring vision in more natural, dynamic settings.

ACKNOWLEDGEMENTS

The authors would like to thank Maëlle Lerebourg and Yana Schwarze for their help with collecting some of the datasets. The work was supported by the Research and Innovation programmes of the European Union (FP7-ICT-270212, H2020-FETPROACT-2014 [H2020 Future and Emerging Technologies] grant SEP-210141273). BE was funded by Deutsche Forschungsgemeinschaft (DFG, German Research Foundation) under Germany's Excellence Strategy - EXC2075 - 390740016. Open Access funding enabled and organized by Projekt DEAL.

CONFLICT OF INTEREST

The authors do not declare any conflict of interest.

AUTHOR CONTRIBUTIONS

Anna L. Gert: Conceptualization; data curation; formal analysis; investigation; methodology; project administration; software; visualizations; writing—original draft preparation; writing—review and editing. **Benedikt V. Ehinger**: Formal analysis; investigation; methodology; software; supervision; writing—review and editing. **Silja Timm**: Data curation; investigation; software. **Tim C. Kietzmann**: Conceptualization; project administration; supervision; writing—review and editing. **Peter König**: Conceptualization; funding acquisition; resources; supervision; writing—review and editing.

PEER REVIEW

The peer review history for this article is available at https://publons.com/publon/10.1111/ejn.15824.

DATA AVAILABILITY STATEMENT

The data and the code to reproduce the results can be found at https://doi.org/10.12751/g-node.ve847p.

ORCID

Anna L. Gert https://orcid.org/0000-0002-7725-1479
Benedikt V. Ehinger https://orcid.org/0000-0002-6276-3332
Tim C. Kietzmann https://orcid.org/0000-0001-8076-6062
Peter König https://orcid.org/0000-0003-3654-5267

REFERENCES

Akaishi, R., Umeda, K., Nagase, A., & Sakai, K. (2014). Autonomous mechanism of internal choice estimate underlies decision inertia. *Neuron*, *81*(1), 195–206. https://doi.org/10.1016/j.neuron.2013.10.018

Amihai, I., Deouell, L. Y., & Bentin, S. (2011). Neural adaptation is related to face repetition irrespective of identity: A reappraisal of the N170 effect. *Experimental Brain Research*, *209*(2), 193–204. https://doi.org/10.1007/s00221-011-2546-x

14609568, 2022, 11, Downloaded from https://onlinelibrary.wiley.com/doi/10.1111/ejn.15824 by Universitatsbibliothek Stuttgart, Wiley Online Library on [27/05/2024]. See the Terms and Conditions (https://onlinelibrary.wiley.com/terms-and-conditions) on Wiley Online Library for rules of use; OA articles are governed by the applicable Creative Commons License

Antonakakis, M., Schrader, S., Aydin, Ü., Khan, A., Gross, J., Zervakis, M., Rampp, S., & Wolters, C. H. (2020). Inter-subject variability of skull conductivity and thickness in calibrated realistic head models. *NeuroImage*, *223*, 117353. https://doi.org/10.1016/j.neuroimage.2020.117353

Auerbach-Asch, C. R., Bein, O., & Deouell, L. Y. (2020). Face selective neural activity: Comparisons between fixed and free viewing. *Brain Topography*, *33*(3), 336–354. https://doi.org/10.1007/s10548-020-00764-7

Bentin, S., Allison, T., Puce, A., Perez, E., & McCarthy, G. (1996). Electrophysiological studies of face perception in humans. *Journal of Cognitive Neuroscience*, *8*(6), 551–565. https://doi.org/10.1162/jocn.1996.8.6.551

Bosch, E., Fritsche, M., Ehinger, B. V., & de Lange, F. P. (2020). Opposite effects of choice history and stimulus history resolve a paradox of sequential choice bias. *Journal of Vision*, *20*(12), 9-9. https://doi.org/10.1167/jov.20.12.9

Buonocore, A., Dimigen, O., & Melcher, D. (2020). Post-saccadic face processing is modulated by pre-saccadic preview: Evidence from fixation-related potentials. *Journal of Neuroscience*, *40*(11), 2305–2313. https://doi.org/10.1523/JNEUROSCI.0861-19.2020

Cauchoix, M., Barragan-Jason, G., Serre, T., & Barbeau, E. J. (2014). The neural dynamics of face detection in the wild revealed by MVPA. *Journal of Neuroscience*, *34*(3), 846–854. https://doi.org/10.1523/JNEUROSCI.3030-13.2014

Cerf, M., Frady, E. P., & Koch, C. (2009). Faces and text attract gaze independent of the task: Experimental data and computer model. *Journal of Vision*, *9*(12), 10. https://doi.org/10.1167/9.12.10

Cornelissen, T., Sassenhagen, J., & Võ, M. L.-H. (2019). Improving free-viewing fixation-related EEG potentials with continuous-time regression. *Journal of Neuroscience Methods*, *313*, 77–94. https://doi.org/10.1016/j.jneumeth.2018.12.010

Dandekar, S., Ding, J., Privitera, C., Carney, T., & Klein, S. A. (2012). The fixation and saccade P3. *PLoS ONE*, *7*(11), e48761. https://doi.org/10.1371/journal.pone.0048761

de Lissa, P., McArthur, G., Hawelka, S., Palermo, R., Mahajan, Y., Degno, F., & Hutzler, F. (2019). Peripheral preview abolishes N170 face-sensitivity at fixation: Using fixation-related potentials to investigate dynamic face processing. *Visual Cognition*, *27*(9–10), 740–759. https://doi.org/10.1080/13506285.2019.1676855

Delorme, A., & Makeig, S. (2004). EEGLAB: An open source toolbox for analysis of single-trial EEG dynamics including independent component analysis. *Journal of Neuroscience Methods*, *134*(1), 9–21. https://doi.org/10.1016/j.jneumeth.2003.10.009

Dering, B., Martin, C. D., Moro, S., Pegna, A. J., & Thierry, G. (2011). Face-sensitive processes one hundred milliseconds after picture onset. *Frontiers in Human Neuroscience*, *5*, 93. https://doi.org/10.3389/fnhum.2011.00093

Dimigen, O. (2020). Optimizing the ICA-based removal of ocular EEG artifacts from free viewing experiments. *NeuroImage*, *207*, 116117. https://doi.org/10.1016/j.neuroimage.2019.116117

Dimigen, O., & Ehinger, B. V. (2021). Regression-based analysis of combined EEG and eye-tracking data: Theory and applications. *Journal of Vision*, *21*(1), 3. https://doi.org/10.1167/jov.21.1.3

Dimigen, O., Sommer, W., Hohlfeld, A., Jacobs, A. M., & Kliegl, R. (2011). Coregistration of eye movements and EEG in natural reading: Analyses and review. *Journal of Experimental Psychology: General*, *140*(4), 552–572. https://doi.org/10.1037/a0023885

Dimigen, O., Sommer, W., & Kliegl, R. (2013). Fixation-related potentials during scene perception. In K. Holmqvist, F. Mulvey, & R. Johannson (Eds.), *Abstracts of the 17th European Conference on Eye Movements 2013: Bd. 6(3) (S. 189)*. Journal of Eye Movement Research. https://doi.org/10.16910/jemr.6.3.1

Ehinger, B. V. (2019). Unmixed: Linear mixed models combined with overlap correction for M/EEG analyses. An extension to the unfold toolbox. In *2019 Conference on Cognitive Computational Neuroscience*. https://doi.org/10.32470/CCN.2019.1102-0

Ehinger, B. V., & Dimigen, O. (2019). Unfold: An integrated toolbox for overlap correction, non-linear modeling, and regression-based EEG analysis. *PeerJ*, *7*, e7838. https://doi.org/10.7717/peerj.7838

Ehinger, B. V., Fischer, P., Gert, A. L., Kaufhold, L., Weber, F., Pipa, G., & König, P. (2014). Kinesthetic and vestibular information modulate alpha activity during spatial navigation: A mobile EEG study. *Frontiers in Human Neuroscience*, *8*, 71. https://doi.org/10.3389/fnhum.2014.00071

Eimer, M. (2011). The face-sensitive N170 component of the event-related brain potential. In A. Calder, G. Rhodes, M. Johnson, & J. Haxby (Eds.), *Oxford handbook of face perception* (Vol. Bd. 28, pp. S. 329–S. 344). Oxford University Press. https://doi.org/10.1093/oxfordhb/9780199559053.013.0017

Fischer, J., & Whitney, D. (2014). Serial dependence in visual perception. *Nature Neuroscience*, *17*(5), 738–743. https://doi.org/10.1038/nn.3689

Ganis, G., Smith, D., & Schendan, H. E. (2012). The N170, not the P1, indexes the earliest time for categorical perception of faces, regardless of interstimulus variance. *NeuroImage*, *62*(3), 1563–1574. https://doi.org/10.1016/j.neuroimage.2012.05.043

George, N., Evans, J., Fiori, N., Davidoff, J., & Renault, B. (1996). Brain events related to normal and moderately scrambled faces. *Cognitive Brain Research*, *4*(2), 65–76. https://doi.org/10.1016/0926-6410(95)00045-3

Gert, A. L., Ehinger, B. V., Kietzmann, T. C., & Konig, P. (2020). Faces strongly attract early fixations in naturally sampled real-world stimulus materials. In *ACM Symposium on Eye Tracking Research and Applications* (pp. 1–5). https://doi.org/10.1145/3379156.3391377

Goffaux, V., Gauthier, I., & Rossion, B. (2003). Spatial scale contribution to early visual differences between face and object processing. *Cognitive Brain Research*, *16*(3), 416–424. https://doi.org/10.1016/S0926-6410(03)00056-9

Handy, T. C. (2005). *Event-related potentials: A methods handbook*. MIT Press.

Hasson, U., Nir, Y., Levy, I., Fuhrmann, G., & Malach, R. (2004). Intersubject synchronization of cortical activity during natural vision. *Science*, *303*(5664), 1634–1640. https://doi.org/10.1126/science.1089506

Hernández-García, A., Gameiro, R. R., Grillini, A., & König, P. (2020). Global visual salience of competing stimuli. *Journal of Vision*, *20*(7), 27. https://doi.org/10.1167/jov.20.7.27

Herrmann, M. J., Ehlis, A.-C., Ellgring, H., & Fallgatter, A. J. (2005). Early stages (P100) of face perception in humans as

14609568, 2022, 11, Downloaded from https://onlinelibrary.wiley.com/doi/10.1111/ejn.15824 by Universitatsbibliothek Stuttgart, Wiley Online Library on [27/05/2024]. See the Terms and Conditions (https://onlinelibrary.wiley.com/terms-and-conditions) on Wiley Online Library for rules of use; OA articles are governed by the applicable Creative Commons License

measured with event-related potentials (ERPs). *Journal of Neural Transmission*, *112*(8), 1073–1081. https://doi.org/10.1007/s00702-004-0250-8

Huber-Huber, C., Buonocore, A., Dimigen, O., Hickey, C., & Melcher, D. (2019). The peripheral preview effect with faces: Combined EEG and eye-tracking suggests multiple stages of trans-saccadic predictive and non-predictive processing. *NeuroImage*, *200*, 344–362. https://doi.org/10.1016/j.neuroimage.2019.06.059

Itier, R. J., & Taylor, M. J. (2004). N170 or N1? Spatiotemporal differences between object and face processing using ERPs. *Cerebral Cortex*, *14*(2), 132–142. https://doi.org/10.1093/cercor/bhg111

Jacques, C., d'Arripe, O., & Rossion, B. (2007). The time course of the inversion effect during individual face discrimination. *Journal of Vision*, *7*(8), 3. https://doi.org/10.1167/7.8.3

Jeffreys, D. A. (1996). Evoked potential studies of face and object processing. *Visual Cognition*, *3*(1), 1–38. https://doi.org/10.1080/713756729

John-Saaltink, E. S., Kok, P., Lau, H. C., & de Lange, F. P. (2016). Serial dependence in perceptual decisions is reflected in activity patterns in primary visual cortex. *Journal of Neuroscience*, *36*(23), 6186–6192. https://doi.org/10.1523/JNEUROSCI.4390-15.2016

Johnston, P., Molyneux, R., & Young, A. W. (2015). The N170 observed 'in the wild': Robust event-related potentials to faces in cluttered dynamic visual scenes. *Social Cognitive and Affective Neuroscience*, *10*(7), 938–944. https://doi.org/10.1093/scan/nsu136

Joyce, C., & Rossion, B. (2005). The face-sensitive N170 and VPP components manifest the same brain processes: The effect of reference electrode site. *Clinical Neurophysiology*, *116*(11), 2613–2631. https://doi.org/10.1016/j.clinph.2005.07.005

Kamienkowski, J. E., Varatharajah, A., Sigman, M., & Ison, M. J. (2018). Parsing a mental program: Fixation-related brain signatures of unitary operations and routines in natural visual search. *NeuroImage*, *183*, 73–86. https://doi.org/10.1016/j.neuroimage.2018.08.010

Kaunitz, L. N., Kamienkowski, J. E., Varatharajah, A., Sigman, M., Quiroga, R. Q., & Ison, M. J. (2014). Looking for a face in the crowd: Fixation-related potentials in an eye-movement visual search task. *NeuroImage*, *89*, 297–305. https://doi.org/10.1016/j.neuroimage.2013.12.006

Kazai, K., & Yagi, A. (2003). Comparison between the lambda response of eye-fixation-related potentials and the P100 component of pattern-reversal visual evoked potentials. *Cognitive, Affective, & Behavioral Neuroscience*, *3*(1), 46–56. https://doi.org/10.3758/CABN.3.1.46

Kietzmann, T. C., Gert, A. L., Tong, F., & König, P. (2016). Representational dynamics of facial viewpoint encoding. *Journal of Cognitive Neuroscience*, *29*(4), 637–651. https://doi.org/10.1162/jocn_a_01070

Konkle, T., & Caramazza, A. (2013). Tripartite organization of the ventral stream by animacy and object size. *Journal of Neuroscience*, *33*(25), 10235–10242. https://doi.org/10.1523/JNEUROSCI.0983-13.2013

Körner, C., Braunstein, V., Stangl, M., Schlögl, A., Neuper, C., & Ischebeck, A. (2014). Sequential effects in continued visual search: Using fixation-related potentials to compare distractor processing before and after target detection. *Psychophysiology*, *51*(4), 385–395. https://doi.org/10.1111/psyp.12062

Kovács, G., Zimmer, M., Bankó, É., Harza, I., Antal, A., & Vidnyánszky, Z. (2006). Electrophysiological correlates of visual adaptation to faces and body parts in humans. *Cerebral Cortex*, *16*(5), 742–753. https://doi.org/10.1093/cercor/bhj020

Krause, J., Stark, M., Deng, J., & Fei-Fei, L. (2013). 3D object representations for fine-grained categorization. In *2013 IEEE International Conference on Computer Vision Workshops* (pp. 554–561). https://doi.org/10.1109/ICCVW.2013.77

Kristensen, E., Rivet, B., & Guérin-Dugué, A. (2017). Estimation of overlapped eye fixation related potentials: The general linear model, a more flexible framework than the ADJAR algorithm. *Journal of Eye Movement Research*, *10*(1), Article 1. https://doi.org/10.16910/jemr.10.1.7

Liberman, A., Fischer, J., & Whitney, D. (2014). Serial dependence in the perception of faces. *Current Biology*, *24*(21), 2569–2574. https://doi.org/10.1016/j.cub.2014.09.025

Liu, J., Harris, A., & Kanwisher, N. (2002). Stages of processing in face perception: An MEG study. *Nature Neuroscience*, *5*(9), 910–916. https://doi.org/10.1038/nn909

Nikolaev, A. R., Meghanathan, R. N., & van Leeuwen, C. (2016). Combining EEG and eye movement recording in free viewing: Pitfalls and possibilities. *Brain and Cognition*, *107*, 55–83. https://doi.org/10.1016/j.bandc.2016.06.004

Nyström, M., & Holmqvist, K. (2010). An adaptive algorithm for fixation, saccade, and glissade detection in eyetracking data. *Behavior Research Methods*, *42*(1), 188–204. https://doi.org/10.3758/BRM.42.1.188

Oliveira, A. S., Schlink, B. R., Hairston, W. D., König, P., & Ferris, D. P. (2016). Induction and separation of motion artifacts in EEG data using a mobile phantom head device. *Journal of Neural Engineering*, *13*(3), 036014. https://doi.org/10.1088/1741-2560/13/3/036014

Palmer, J. A., Kreutz-Delgado, K., & Makeig, S. (2012). *AMICA: An adaptive mixture of independent component analyzers with shared components*. Swartz Center for Computatonal Neursoscience, University of California San Diego, Tech. Rep.

Pernet, C. R., Wilcox, R. R., & Rousselet, G. A. (2013). Robust correlation analyses: False positive and power validation using a new open source Matlab toolbox. *Frontiers in Psychology*, *3*. https://doi.org/10.3389/fpsyg.2012.00606

Peterson, M. F., Lin, J., Zaun, I., & Kanwisher, N. (2016). Individual differences in face-looking behavior generalize from the lab to the world. *Journal of Vision*, *16*(7), 12. https://doi.org/10.1167/16.7.12

Plöchl, M., Ossandón, J. P., & König, P. (2012). Combining EEG and eye tracking: Identification, characterization, and correction of eye movement artifacts in electroencephalographic data. *Frontiers in Human Neuroscience*, *6*, 278. https://doi.org/10.3389/fnhum.2012.00278

Retter, T. L., & Rossion, B. (2016). Uncovering the neural magnitude and spatio-temporal dynamics of natural image categorization in a fast visual stream. *Neuropsychologia*, *91*, 9–28. https://doi.org/10.1016/j.neuropsychologia.2016.07.028

Rossion, B., & Caharel, S. (2011). ERP evidence for the speed of face categorization in the human brain: Disentangling the contribution of low-level visual cues from face perception. *Vision Research*, *51*(12), 1297–1311. https://doi.org/10.1016/j.visres.2011.04.003

14609568, 2022, 11, Downloaded from https://onlinelibrary.wiley.com/doi/10.1111/ejn.15824 by Universitatsbibliothek Stuttgart, Wiley Online Library on [27/05/2024]. See the Terms and Conditions (https://onlinelibrary.wiley.com/terms-and-conditions) on Wiley Online Library for rules of use; OA articles are governed by the applicable Creative Commons License

Rossion, B., Gauthier, I., Tarr, M. J., Despland, P., Bruyer, R., Linotte, S., & Crommelinck, M. (2000). The N170 occipito-temporal component is delayed and enhanced to inverted faces but not to inverted objects: An electrophysiological account of face-specific processes in the human brain. *Neuroreport*, *11*(1), 69–72. https://doi.org/10.1097/00001756-200001170-00014

Rossion, B., & Jacques, C. (2008). Does physical interstimulus variance account for early electrophysiological face sensitive responses in the human brain? Ten lessons on the N170. *NeuroImage*, *39*(4), 1959–1979. https://doi.org/10.1016/j.neuroimage.2007.10.011

Rousselet, G. (2012). Does filtering preclude us from studying ERP time-courses? *Frontiers in Psychology*, *3*, 131. https://doi.org/10.3389/fpsyg.2012.00131

Rousselet, G. A., Husk, J. S., Bennett, P. J., & Sekuler, A. B. (2008). Time course and robustness of ERP object and face differences. *Journal of Vision*, *8*(12), 3. https://doi.org/10.1167/8.12.3

Rousselet, G. A., Macé, M. J.-M., & Fabre-Thorpe, M. (2004). Animal and human faces in natural scenes: How specific to human faces is the N170 ERP component? *Journal of Vision*, *4*(1), 2. https://doi.org/10.1167/4.1.2

Sadeh, B., Podlipsky, I., Zhdanov, A., & Yovel, G. (2010). Event-related potential and functional MRI measures of face-selectivity are highly correlated: A simultaneous ERP-fMRI investigation. *Human Brain Mapping*, *31*(10), 1490–1501. https://doi.org/10.1002/hbm.20952

Schönbrodt, F. D., & Perugini, M. (2013). At what sample size do correlations stabilize? *Journal of Research in Personality*, *47*(5), 609–612. https://doi.org/10.1016/j.jrp.2013.05.009

Schweinberger, S. R., & Neumann, M. F. (2016). Repetition effects in human ERPs to faces. *Cortex*, *80*, 141–153. https://doi.org/10.1016/j.cortex.2015.11.001

Smith, N. J., & Kutas, M. (2015). Regression-based estimation of ERP waveforms: II. Nonlinear effects, overlap correction, and practical considerations. *Psychophysiology*, *52*(2), 169–181. https://doi.org/10.1111/psyp.12320

Soto, V., Tyson-Carr, J., Kokmotou, K., Roberts, H., Cook, S., Fallon, N., Giesbrecht, T., & Stancak, A. (2018). Brain responses to emotional faces in natural settings: A wireless mobile EEG recording study. *Frontiers in Psychology*, *9*, 2003. https://doi.org/10.3389/fpsyg.2018.02003

SR Research (2009). *EyeLink 1000 user manual, v.1.5.0*. Mississauga, ON: SR Research Ltd.

Summerfield, C., Wyart, V., Mareike Johnen, V., & de Gardelle, V. (2011). Human scalp electroencephalography reveals that repetition suppression varies with expectation. *Frontiers in Human Neuroscience*, *5*, 67. https://doi.org/10.3389/fnhum.2011.00067

Tatler, B. W. (2007). The central fixation bias in scene viewing: Selecting an optimal viewing position independently of motor biases and image feature distributions. *Journal of Vision*, *7*(14), 4. https://doi.org/10.1167/7.14.4

Thierry, G., Martin, C. D., Downing, P., & Pegna, A. J. (2007). Controlling for interstimulus perceptual variance abolishes N170 face selectivity. *Nature Neuroscience*, *10*(4), 505–511. https://doi.org/10.1038/nn1864

Urai, A. E., Braun, A., & Donner, T. H. (2017). Pupil-linked arousal is driven by decision uncertainty and alters serial choice bias. *Nature Communications*, *8*(1), 1–11. https://doi.org/10.1038/ncomms14637

Weiner, K. S., & Grill-Spector, K. (2013). Neural representations of faces and limbs neighbor in human high-level visual cortex: Evidence for a new organization principle. *Psychological Research*, *77*(1), 74–97. https://doi.org/10.1007/s00426-011-0392-x

Widmann, A., Schröger, E., & Maess, B. (2015). Digital filter design for electrophysiological data—A practical approach. *Journal of Neuroscience Methods*, *250*, 34–46. https://doi.org/10.1016/j.jneumeth.2014.08.002

Wilkinson, G. N., & Rogers, C. E. (1973). Symbolic description of factorial models for analysis of variance. *Journal of the Royal Statistical Society: Series C: Applied Statistics*, *22*(3), 392–399. https://doi.org/10.2307/2346786

Wilming, N., Harst, S., Schmidt, N., & König, P. (2013). Saccadic momentum and facilitation of return saccades contribute to an optimal foraging strategy. *PLoS Computational Biology*, *9*(1), e1002871. https://doi.org/10.1371/journal.pcbi.1002871

Yarkoni, T. (2019). The generalizability crisis. *Behavioral and Brain Sciences*, *45*, E1. https://doi.org/10.1017/S0140525X20001685

SUPPORTING INFORMATION

Additional supporting information can be found online in the Supporting Information section at the end of this article.

How to cite this article: Gert, A. L., Ehinger, B. V., Timm, S., Kietzmann, T. C., & König, P. (2022). WildLab: A naturalistic free viewing experiment reveals previously unknown electroencephalography signatures of face processing. *European Journal of Neuroscience*, *56*(11), 6022–6038. https://doi.org/10.1111/ejn.15824

14609568, 2022, 11, Downloaded from https://onlinelibrary.wiley.com/doi/10.1111/ejn.15824 by Universitatsbibliothek Stuttgart, Wiley Online Library on [27/05/2024]. See the Terms and Conditions (https://onlinelibrary.wiley.com/terms-and-conditions) on Wiley Online Library for rules of use; OA articles are governed by the applicable Creative Commons License